

# Surface and Bulk Electronic Structure of the Strongly Correlated System $\text{SmB}_6$ and Implications for a Topological Kondo Insulator

N. Xu,<sup>1,\*</sup> X. Shi,<sup>1,2</sup> P. K. Biswas,<sup>3</sup> C. E. Matt,<sup>1,4</sup> R. S. Dhaka,<sup>1</sup> Y. Huang,<sup>1</sup> N. C. Plumb,<sup>1</sup> M. Radović,<sup>1,5</sup> J. H. Dil,<sup>6,1</sup> E. Pomjakushina,<sup>7</sup> A. Amato,<sup>3</sup> Z. Salman,<sup>3</sup> D. McK. Paul,<sup>8</sup> J. Mesot,<sup>1,9</sup> H. Ding,<sup>2</sup> and M. Shi<sup>1,†</sup>

<sup>1</sup>*Swiss Light Source, Paul Scherrer Institut, CH-5232 Villigen PSI, Switzerland*

<sup>2</sup>*Beijing National Laboratory for Condensed Matter Physics, and Institute of Physics, Chinese Academy of Sciences, Beijing 100190, China*

<sup>3</sup>*Laboratory for Muon Spin Spectroscopy, Paul Scherrer Institut, CH-5232 Villigen PSI, Switzerland*

<sup>4</sup>*Laboratory for Solid State Physics, ETH Zürich, CH-8093 Zürich, Switzerland*

<sup>5</sup>*SwissFEL, Paul Scherrer Institut, CH-5232 Villigen PSI, Switzerland*

<sup>6</sup>*Physik-Institut, Universität Zürich, Winterthurerstrass 190, CH-8057 Zürich, Switzerland*

<sup>7</sup>*Laboratory for Developments and Methods, Paul Scherrer Institut, CH-5232 Villigen PSI, Switzerland*

<sup>8</sup>*Physics Department, University of Warwick, Coventry, CV4 7AL, United Kingdom*

<sup>9</sup>*Institut de la Matière Complexe, EPF Lausanne, CH-1015, Lausanne, Switzerland*

(Dated: September 21, 2018)

Recent theoretical calculations and experimental results suggest that the strongly correlated material  $\text{SmB}_6$  may be a realization of a topological Kondo insulator. We have performed an angle-resolved photoemission spectroscopy study on  $\text{SmB}_6$  in order to elucidate elements of the electronic structure relevant to the possible occurrence of a topological Kondo insulator state. The obtained electronic structure in the whole three-dimensional momentum space reveals one electron-like  $5d$  bulk band centred at the X point of the bulk Brillouin zone that is hybridized with strongly correlated  $f$  electrons, as well as the opening of a Kondo bandgap ( $\Delta_B \sim 20$  meV) at low temperature. In addition, we observe electron-like bands forming three Fermi surfaces at the center  $\bar{\Gamma}$  point and boundary  $\bar{X}$  point of the surface Brillouin zone. These bands are not expected from calculations of the bulk electronic structure, and their observed dispersion characteristics are consistent with surface states. Our results suggest that the unusual low-temperature transport behavior of  $\text{SmB}_6$  is likely to be related to the pronounced surface states sitting inside the band hybridisation gap and/or the presence of a topological Kondo insulating state.

PACS numbers: 73.20.-r, 71.20.-b, 75.70.Tj, 79.60.-i

A three-dimensional (3D) topological insulator (TI) is an unusual topological quantum state associated with unique metallic surface states that appear within the bulk bandgap [1, 2]. Owing to the peculiar spin texture protected by time-reversal symmetry, the Dirac fermions in TIs are forbidden from scattering due to nonmagnetic impurities and disorder [3, 4]. Hence they carry dissipationless spin current [5], making it possible to explore fundamental physics, spintronics, and quantum computing [1, 2]. However, even after extensive materials synthesis efforts [6–10], impurities in the bulk of these materials make them metallic, prompting us to search for new types of TIs with truly insulating bulks.

The 3D Kondo insulator  $\text{SmB}_6$  may open a new route to realizing topological surface states.  $\text{SmB}_6$  is a typical heavy fermion material with strong electron correlation. Localized  $f$  electrons hybridize with conduction electrons, leading to a narrow bandgap on the order of 10 meV opening at low temperatures, with the chemical potential lying in the gap [11–14]. Due to the opening of the bandgap, the conductivity changes from metallic to insulating behavior with decreasing temperature. It saturates to a constant value below about 1 K, which is thought to be caused by in-gap states [15]. Theoretical studies have proposed that  $\text{SmB}_6$  may host three-

dimensional topological insulating phases [16, 17]. Recently, transport experiments employing a novel geometry [18] showed convincing evidence of a distinct surface contribution to the conductivity that is unmixed with the bulk contribution, suggesting  $\text{SmB}_6$  is an ideal topological insulator with a perfectly insulating bulk. Point-contact spectroscopy revealed that the low-temperature Kondo insulating state harbors conduction states on the surface, in support of predictions of nontrivial topology in Kondo insulators [19]. Moreover, Lu et al. used the local density approximation combined with the Gutzwiller method to investigate the topological physics of  $\text{SmB}_6$  from the first principles [17]. They found a nontrivial  $\mathbb{Z}_2$  topology, indicating that  $\text{SmB}_6$  is a strongly correlated topological insulator. They calculated the topological surface states, and found three Dirac cones, in contrast to most known topological insulators. At present, topological insulators are essentially understood within the theory of non-interacting topological theory [1, 2].  $\text{SmB}_6$ , as one candidate for a topological Kondo insulator, potentially offers us an opportunity to investigate the interplay between topological states and strong many-body interactions.

As a surface-sensitive technique, angle-resolved photoemission spectroscopy (ARPES) is one of the best

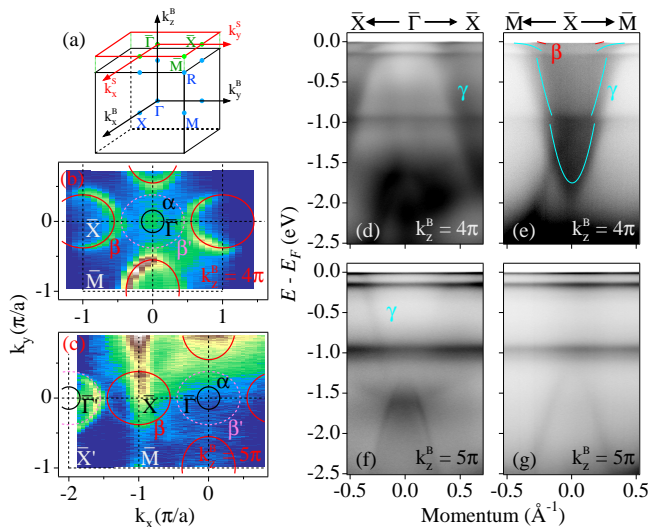


FIG. 1. (Color online): (a) The first Brillouin zone of  $\text{SmB}_6$  and the projection on the cleaving surface. High-symmetry points are also indicated. (b),(c) Fermi surface mapping at  $T = 17$  K by integrating ARPES intensity within  $E_F \pm 5$  meV with  $h\nu = 26$  and  $46$  eV, corresponding  $k_z = 4\pi$  and  $5\pi$  at  $\bar{\Gamma}$ , respectively. (d),(e) ARPES intensity plots at  $\bar{\Gamma}$  and  $\bar{X}$  for the  $k_z^B = 4\pi$  plane at  $T = 17$  K. The red and blue curves are the dispersions of the  $\beta$  and  $\gamma$  bands extracted by MDC fitting. (f),(g) Analogous to (d),(e), but for the  $k_z^B = 5\pi$  plane.

probes to investigate the surface states and attest to their topological nature. However, previous ARPES studies did not resolve the surface dispersion from bulk states, possibly due to the system resolution and sample surface condition [20, 21]. In this letter, we report high-resolution ARPES results from  $\text{SmB}_6$  in the whole three-dimensional Brillouin zone (BZ) by tuning the incident photon energy. Due to the high resolution of the ARPES system and good sample quality, we are able for the first time to clearly identify electron-like bands forming three Fermi surfaces (FS), which are distinct from the expected bulk states, and we discuss the possible topological property of those surface states.

High quality single crystals of  $\text{SmB}_6$  were grown by the flux method. ARPES measurements were performed at the Surface/Interface Spectroscopy (SIS) beamline at the Swiss Light Source using a VG-Scienta R4000 electron analyzer with photon energies ranging from 22 to 110 eV. The energy resolution ranged from  $\sim 10$  meV at 22 eV to  $\sim 15$  meV at 110 eV. The angular resolution was around  $0.2^\circ$ . Clean surfaces for the ARPES measurements were obtained by cleaving the crystals *in situ* in a working vacuum better than  $5 \times 10^{-11}$  Torr. Shiny mirror-like surfaces were obtained after cleaving the samples, confirming their high quality.

Fig. 1 displays the Fermi surface and band dispersions of  $\text{SmB}_6$  measured at  $T = 17$  K with various photon energies, corresponding to different  $k_z$  points in the bulk

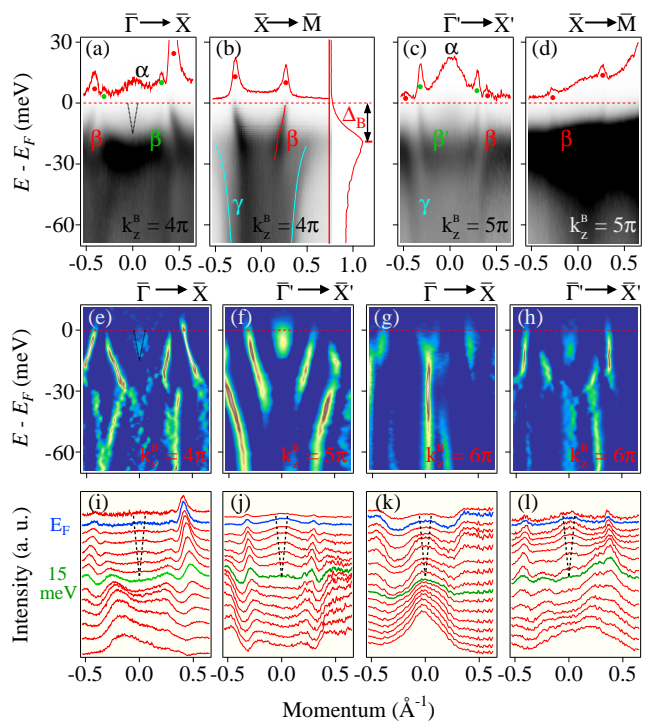


FIG. 2. (Color online) (a),(b) ARPES intensity plots for cuts through  $\bar{\Gamma} - \bar{X}$  and  $\bar{X} - \bar{M}$ , respectively, for the  $k_z^B = 4\pi$  plane. Note the narrow energy window. The data were collected at  $T = 17$  K. The red and blue curves are dispersions for the  $\beta$  and  $\gamma$  bands extracted by fitting the MDCs. The curves on the top are the MDCs taken at  $E_F$ , with labels for the peak positions. An EDC at the location in  $k$  space marked by the red vertical line is also displayed. From this, the Kondo bandgap is estimated to be  $\Delta_B \sim 20$  meV. (c),(d) Analogous to (a),(b), but for the  $k_z^B = 5\pi$  plane. (e)-(g) Plots of the curvatures of the MDC intensities along  $\bar{\Gamma} - \bar{X}$  in either the first or second BZ ( $\bar{\Gamma}' - \bar{X}'$ ) evaluated in the  $k_z^B = 4\pi$ ,  $5\pi$  and  $6\pi$  planes, respectively. (h) MDC curvature analysis at the second BZ center  $\bar{\Gamma}'$  point for the  $k_z^B = 6\pi$  plane. (i)-(l) Corresponding MDC plots for (e)-(h).

BZ ( $k_z^B$ ). The first BZ of bulk  $\text{SmB}_6$  and its projection on the cleaving surface are shown in Fig. 1 (a), with all the high symmetry points labeled. In Figs. 1 (b) and (c), we plot the FS mappings obtained using  $h\nu = 26$  and  $46$  eV, corresponding to approximately  $k_z^B = 4\pi$  and  $5\pi$ , allowing direct comparisons with previous work [20, 21]. In making the maps, we integrated the ARPES intensity within  $E_F \pm 5$  meV. As seen in Figs. 1 (b) and (c), the same FS topology is observed at different  $k_z^B$  high symmetry points of the bulk BZ: one small circular FS,  $\alpha$ , is located at the surface BZ center  $\bar{\Gamma}$  point and an additional ellipse-shaped FS,  $\beta$ , is located at the surface BZ boundary  $\bar{X}$  point. We also observed a folded band  $\beta'$  caused by a  $1 \times 2$  reconstruction of the surface, which is also observed in low-energy electron diffraction (LEED) patterns [20]. Figs. 1 (d) and (e) show photoemission  $E$ -vs- $k$  intensity plots at the  $\bar{\Gamma}$  and  $\bar{X}$  points for the  $k_z^B$

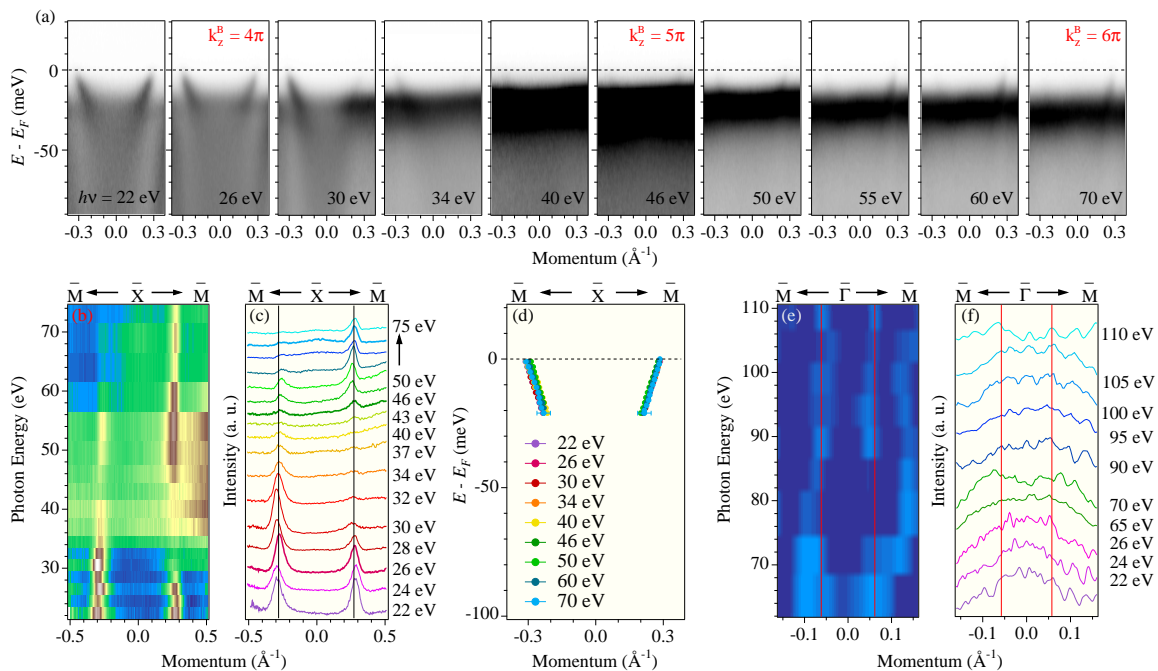


FIG. 3. (Color online) (a) ARPES intensity along the  $\bar{X} - \bar{M}$  direction measured at  $T = 17$  K with various photon energies. (b) Plot of the ARPES intensity along  $\bar{X} - \bar{M}$  as a function of photon energies from 22 eV to 75 eV, covering more than 1.5 BZs along  $k_z^B$ . (c) Corresponding MDCs at  $E_F$ . (d) Extracted dispersions of the  $\beta$  band for different photon energies. (e) Plot of the curvature of the MDC intensity along  $\bar{\Gamma} - \bar{M}$  for each photon energy. (f) Corresponding MDCs at  $E_F$ .

$= 4\pi$  plane at  $T = 17$  K. Similarly, data recorded for the  $k_z^B = 5\pi$  plane are shown in Figs. 1 (f) and (g). One can see that the highly renormalized  $4f^6$  electrons form three flat bands, located at  $E_B = 960, 160$  and  $20$  meV. One electron-like band,  $\gamma$ , hybridizes with three  $4f^6$  bands at low temperature. The  $\gamma$  band, which is attributed to the  $5d$  orbital as suggested by [17], is seen at  $\bar{X}$  for  $k_z^B = 4\pi$  and at  $\bar{\Gamma}$  for  $k_z^B = 5\pi$ , which in the bulk BZ are equivalent at the  $X$  point, as seen in Fig. 1 (a). This strongly three-dimensional feature indicates that  $\gamma$  is a bulk band located at the  $X$  point in the bulk BZ, consistent with the theoretical calculation [17].

In order to investigate the low energy excitations, band dispersions near  $E_F$  at  $\bar{\Gamma}$  and  $\bar{X}$  for the  $k_z^B = 4\pi$  plane are shown in Figs. 2 (a) and (b). In addition, we plot the ARPES intensity near  $E_F$  at the center of the second surface BZ  $\bar{\Gamma}'$  point and  $\bar{X}$  point for the  $k_z^B = 5\pi$  plane in Figs. 2 (d) and (e). As seen in Figs. 2 (b) and (d), the bulk band  $\gamma$  hybridizes with the flat  $4f$  band near  $E_F$ , leading to a Kondo bandgap. The gap size is  $\Delta_B \sim 20$  meV based on the peak position of the energy distribution curve (EDC) taken at the position marked by the vertical red line in Fig. 2 (b). Moreover, as seen in Figs. 2 (b) and (d), the electron-like band  $\beta$  appears inside the bandgap and crosses  $E_F$  at the  $\bar{X}$  point, forming an ellipse-shaped FS at the BZ boundary. For the  $\beta$  band, its Fermi momentum  $k_F$  measures  $0.39$  and  $0.28 \text{ \AA}^{-1}$  along the  $\bar{X} - \bar{\Gamma}$  and  $\bar{X} - \bar{M}$  directions, respectively. The

folded band  $\beta'$  can be seen in Figs. 2 (a) and (c), located about at  $\bar{\Gamma}$ , with a folding wave vector  $(\pi, 0)$  caused by the  $1 \times 2$  surface reconstruction. Additionally, we observe one weak band  $\alpha$  at the  $\bar{\Gamma}$  point, which corresponds to the small FS at the BZ center. To better visualize the weak  $\alpha$  band, in Figs. 2 (e)-(h) we plot the curvature of the MDC intensity [22] along  $\bar{\Gamma} - \bar{M}$  for different photon energies approximately corresponding to the  $k_z^B = 4\pi, 5\pi$  and  $6\pi$  planes. The corresponding raw momentum distribution curves (MDCs) are also plotted in Figs. 2 (i)-(l). From the curvature plots, we can see that the electron-like  $\alpha$  band crosses  $E_F$  around the  $\bar{\Gamma}$  point, which can be also observed in the MDCs plots. The MDCs at  $E_F$  in Figs. 2 (a) and (c) confirm that the  $\alpha$  and  $\beta$  bands indeed cross  $E_F$ .

From bulk band calculations [16, 17], the in-gap bands  $\alpha$  and  $\beta$  are totally unexpected at any  $k_z^B$  value. However, both theoretical and experimental results [16–19] suggest that  $\text{SmB}_6$  exhibits metallic surface states that make it a candidate for a strongly correlated Kondo topological insulator. To further examine whether the in-gap states are surface or bulk bands, we have carried out an ARPES measurement along the cut crossing the  $\bar{X}$  point for different  $k_z^B$  values by tuning photon energy. In Fig. 3 (a) we plot ARPES spectra with  $k_{\parallel}$  oriented along the  $\bar{X} - \bar{M}$  line taken with different photon energies from 22 to 70 eV, which cover more than 1.5 bulk BZs along  $k_z^B$ . One can see that, although the spectral weight of

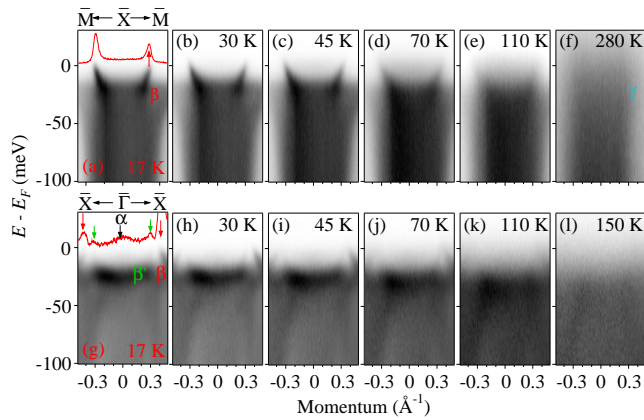


FIG. 4. (Color online) (a)-(f) ARPES intensity plots along  $\bar{M} - \bar{X} - \bar{M}$  measured at  $T = 17$  K, 30 K, 45 K, 70 K, 110 K and 280 K, respectively. (g)-(l) ARPES intensity plots along  $\bar{X} - \bar{\Gamma} - \bar{X}$  measured at  $T = 17$  K, 30 K, 45 K, 70 K, 110 K and 150 K, respectively.

the  $\beta$  band varies with photon energy due to photoemission matrix element effects, the dispersion of the  $\beta$  band stays highly fixed. MDCs at  $E_F$  obtained with different photon energies are plotted in Fig. 3 (c), and the corresponding  $h\nu - k_{\parallel}$  FS intensity plot is shown in Fig. 3 (b). As one immediately recognizes from Fig. 3 (c), the peak position of the MDCs at  $E_F$ , which indicate the  $k_F$  values of the  $\beta$  band, are stationary with respect to  $h\nu$ . Thus the  $\beta$  band forms a two-dimensional FS in the  $h\nu - k_{\parallel}$  plane shown in Fig. 3 (b). In fact, when we plot the extracted dispersions for different photon energies in Fig. 3 (d), their linear dispersions overlap each other within the experimental uncertainties, demonstrating the two-dimensional nature of the  $\beta$  band. This two-dimensional feature is different from the bulk  $\gamma$  band, indicating the surface origin of the  $\beta$  band. We likewise studied the photon energy dependence of the small  $\alpha$  band to check its surface/bulk origin. While the weak intensity and shallow dispersion make detailed quantitative analysis of the  $\alpha$  band difficult, we consistently find anomalous spectral weight at  $E_F$  connected to this band, independent of the photon energy. This is consistent with a shallow 2D state that is nondispersive along  $k_z$ . In light of the fact that the  $\alpha$  band is not predicted from bulk band structure calculations, the data strongly suggest that the  $\alpha$  band, like the  $\beta$  band, has a surface origin.

We have also performed temperature dependent measurements to study the evolution of both the bulk and surface bands. Figs. 4 (a)-(f) show ARPES intensity plots at the  $\bar{X}$  point measured at temperatures ranging from 17 to 280 K. Figs. 4 (g)-(i) show similar plots at the  $\bar{\Gamma}$  point measured at temperatures ranging from 17 to 150 K. The hybridization between the  $5d$   $\gamma$  band and  $4f$  flat band is destroyed around  $T = 110$  K. Meanwhile, the surface bands  $\alpha$  and  $\beta$ , as well as the folding band  $\beta'$ ,

vanish. The temperature dependence suggests that the surface states can only exist when the Kondo bandgap opens.

Our ARPES results demonstrate that  $\text{SmB}_6$  is a strongly correlated Kondo insulator with metallic surface states located inside the Kondo bandgap. The observed surface bands at both the  $\bar{\Gamma}$  and  $\bar{X}$  points show good agreement with the topologically non-trivial surface states found in calculations [17], suggesting that  $\text{SmB}_6$  is a topological Kondo insulator as predicted theoretically [16, 17]. Three surface bands ( $\alpha$  contributes one FS at the  $\bar{\Gamma}$  point and  $\beta$  contributes two FSs at the  $\bar{X}$  point) enclose an odd number of time-reversal-invariant momenta, which is a very strong indication of a topological non-trivial phase. We also note that no clear Dirac point is observed in our ARPES measurements; for the  $\alpha$  band, the intensity is too dim to see a potential Dirac point clearly. One possible reason is that the cleaving surface is the B-terminated layer, and the  $\alpha$  band may originate from Sm, making the signal very weak. For the  $\beta$  band, the intensity diminishes suddenly at  $E_B \sim 20$  meV, corresponding to the hybridization gap edge between  $f$  and  $d$  electrons, which may prohibit observing the Dirac point formed by the bands crossing each other. Thus the apparent absence of a clear Dirac point may be a signature of interactions between topological surface states and the strongly correlated bulk  $f$  electrons. Such non-trivial many-body interactions have recently been observed in other topological insulators studied by ARPES [23]. This hints that  $\text{SmB}_6$  may offer an opportunity to understand topological insulators beyond the noninteracting topological theory.

In summary, we reported high resolution ARPES results from the strongly correlated Kondo insulator  $\text{SmB}_6$ . We first identified two anomalous bands,  $\alpha$  located at the BZ center  $\bar{\Gamma}$  and two  $\beta$  the BZ boundary  $\bar{X}$ , respectively, that are distinct from the expected bulk band structure. While the shallow dispersion of the  $\alpha$  band prevents clear analysis of its shape as a function of  $k_z$ , we managed to explicitly show that the  $\beta$  band is a 2D surface state. The observation of these states agrees well with the topologically non-trivial surface states predicted by theory calculations [16, 17]. We also observe that the  $\alpha$  and  $\beta$  bands disappear when the hybridization between the bulk  $\gamma$  band and the heavily correlated  $f$  electrons vanishes at high temperature. Our results uphold the possibility that  $\text{SmB}_6$  is a topological Kondo insulator, consistent with theoretical calculations [16, 17].

## ACKNOWLEDGMENTS

We acknowledge Z. Fang for stimulating discussions. This work was mainly supported by the Sino-Swiss Science and Technology Cooperation (Project No. IZLCZ2138954). This work was also supported by grants

from MOST (2010CB923000), NSFC. This work is based in part upon research conducted at the Swiss Light Source of the Paul Scherrer Institut in Villigen, Switzerland, and we thank the SIS beamline staff for their excellent support.

---

\* nan.xu@psi.ch

† ming.shi@psi.ch

- [1] M. Z. Hasan and C. L. Kane, *Rev. Mod. Phys.* **82**, 3045 (2010)
- [2] X. L. Qi and S.C. Zhang, *Rev. Mod. Phys.* **83**, 1057 (2011)
- [3] Y. Xia *et al.*, *Nat. Phys.* **5**, 398 (2009)
- [4] S. Souma *et al.*, *Phys. Rev. Lett.* **106**, 216803 (2011)
- [5] C. L. Kane and E. J. Mele, *Science* **314**, 1692 (2006)
- [6] H. Peng *et al.*, *Nat. Mater.* **9**, 225 (2009)
- [7] J. G. Checkelsky, Y. S. Hor, R. J. Cava and N. P. Ong, *Phys. Rev. Lett.* **106**, 196801 (2011)
- [8] J. Checkelsky *et al.*, *Nat. Phys.* **6**, 960 (2010)
- [9] A. A. Taskin and Y. Ando, *Phys. Rev. B* **80**, 085303 (2009)
- [10] D. Kim *et al.*, *Nat. Phys.* **8**, 460 (2012)
- [11] P. Coleman, *Handbook of Magnetism and Advanced Magnetic Materials* **1**, 95 (2007)
- [12] G. Aeppli and Z. Fisk, *Comments Condens. Matter Phys.* **16**, 155 (1992)
- [13] H. Tsunetsugu, M. Sigrist, and K. Ueda, *Rev. Mod. Phys.* **69**, 809 (1997)
- [14] P. Riseborough,, *Adv. Phys.* **49**, 257 (2000)
- [15] A. Menth, E. Buehler, and T.H. Geballe, *Phys. Rev. Lett.* **22**, 295 (1969)
- [16] M. Dzero, K. Sun, V. Galitski and P. Coleman, *Phys. Rev. Lett.* **104**, 106408 (2010)
- [17] F. Lu, J. Z. Zhao, H. Weng, Z. Fang and X. Dai, *Phys. Rev. Lett.* **110**, 096401 (2013)
- [18] J. Botimer *et al.*, arXiv, 1211.6769(2012)
- [19] X. H. Zhang *et al.*, *Phys. Rev. X* **3**, 011011 (2013)
- [20] H. Miyazaki, T. Hajiri, T. Ito, S. Kunii and S. I. Kimura, *Phys. Rev. B* **86**, 075105 (2012)
- [21] J. D. Denlinger *et al.*, *Physica B* **281-282**, 716 (2000)
- [22] P. Zhang *et al.*, *Rev. Sci. Instrum.* **82**, 043712 (2011)
- [23] T. Kondo *et al.*, *Phys. Rev. Lett.* **110**, 217601 (2013)